62 *Inorg. Chem.* **2010**, *49*, 62–72
DOI: 10.1021/ic901100z

Inorganic Chemistry
Article

Factors Dictating the Nuclearity/Aggregation and Acetate Coordination Modes of Lutidine-Coordinated Zinc(II) Acetate Complexes

Umesh Kumar,[†] Jency Thomas,[‡] and Natesan Thirupathi*,[†]

[†]*Department of Chemistry, University of Delhi, Delhi − 110 007, India and* [‡]*Department of Chemistry, Indian Institute of Technology Delhi, Delhi − 110 016, India*

Received June 9, 2009

The reactions of $Zn(OAc)_2 \cdot 2H_2O$ with various positional isomers of lutidine were explored with a view to understand the factors responsible for the nuclearity/aggregation and acetate coordination modes of the products. The reactions of $Zn(OAc)_2 \cdot 2H_2O$ with 3,5-lutidine, 2,3-lutidine, 2,4-lutidine, and 3,4-lutidine in a 1:1 ratio in methanol at ambient temperature afforded three discrete trinuclear complexes $[Zn_3(OAc)_2(\mu_2\text{-}\eta^2\text{:}\eta^1\text{-OAc})_2(\mu_2\text{-}\eta^1\text{:}\eta^1\text{-OAc})_2(H_2O)_2(3,5\text{-lutidine})_2]$ (**1**), $[Zn_3(\mu_2\text{-}\eta^1\text{:}\eta^1\text{-OAc})_4(\mu_2\text{-}\eta^2\text{:}\eta^0\text{-OAc})_2L_2]$ [L = 2,3-lutidine (**2**) and 2,4-lutidine (**3**)], and a one-dimensional coordination polymer $[Zn(OAc)(\mu_2\text{-}\eta^1\text{:}\eta^1\text{-OAc})(3,4\text{-lutidine})]$ (**4**) in 93, 79, 81, and 94% yields, respectively. Complexes **1**−**4** were characterized by microanalytical, IR, solution (^1H and ^{13}C), and solid-state cross-polarization magic angle spinning ^{13}C NMR spectroscopic techniques and single-crystal X-ray diffraction data. Complex **1** is unique in that it contains three types of acetate coordination modes, namely, monodentate, bridging bidentate, and asymmetric chelating bridging. Variable-temperature ^1H NMR data indicated that complex **1** partially dissociates in solution, and the remaining undissociated **1** undergoes a rapid "carboxylate shift" even at 218 K. The plausible mechanism of formation of complexes **1**−**4** was explained with the aid of a point zero charge (pzc) model, according to which the nuclearity/aggregation observed in complexes **1**−**4** depends upon the number and nature of equilibrating species formed upon dissolution of the reactants in methanol, and these in turn depend upon the subtle basic/steric properties of lutidines. Further, noncovalent interactions play a crucial role in determining the nuclearity/aggregation and acetate coordination modes of the products.

Introduction

Lewis base coordinated zinc(II) carboxylate complexes are an important class of coordination compounds due to their relevance as structural and functional models for biologically important metalloenzymes,[1] as Lewis acid catalysts for the copolymerization of cyclohexene oxide and carbon dioxide to afford polycarbonates,[2] and as useful precursors for nano-sized ZnO.[3] Further, complex frameworks present in some of the Lewis base coordinated zinc(II) carboxylate complexes are frequently observed as a fundamental building blocks or secondary building units in zinc(II) carboxylate based metal organic frameworks (MOFs).[4] Anionic carboxylates are highly flexible and versatile *O*-donor ligands in that a range of substituents may be introduced on the carbonyl carbon to modulate its reactivity and coordination propensity to result in a variety of coordination modes such as monodentate, chelating, bidentate bridging, monoatomic bridging, and chelating bridging, as depicted in Figure 1.[5]

*To whom correspondence should be addressed. E-mail: tnat@chemistry.du.ac.in, thirupathi_n@yahoo.com.

(1) (a) Weston, J. *Chem. Rev.* **2005**, *105*, 2151. (b) Lippard, S. J.; Berg, J. M. *Principle of Bio-inorganic Chemistry*; Panima Publishing Corporation: New Delhi, India, 2005. (c) Parkin, G. *Chem. Rev.* **2004**, *104*, 699. (d) Brown, D. A.; Errington, W.; Fitzpatrick, N. J.; Glass, W. K.; Kemp, T. J.; Nimir, H.; Ryan, A. T. *Chem. Commun.* **2002**, 1210. (e) Lipscomb, W. N.; Sträter, N. *Chem. Rev.* **1996**, *96*, 2375. (f) Wilcox, D. E. *Chem. Rev.* **1996**, *96*, 2435. (g) Chen, X-M.; Tong, Y-X. *Inorg. Chem.* **1994**, *33*, 4586. (h) Vallee, B. L.; Alud, D. S. *Acc. Chem. Res.* **1993**, *26*, 543.

(2) Darensbourg, D. J.; Wildeson, J. R.; Yarbrough, J. C. *Inorg. Chem.* **2002**, *41*, 973.

(3) Cingolani, A.; Galli, S.; Masciocchi, N.; Pandolfo, L.; Pettinari, C.; Sironi, A. *Dalton Trans.* **2006**, 2479.

(4) (a) Qi, Y.; Che, Y.-X.; Zheng, J.-M. *Cryst. Eng. Comm.* **2008**, *10*, 1137. (b) Burrows, A. D.; Frost, C. G.; Mahon, M. F.; Richardson, C. *Angew. Chem., Int. Ed.* **2008**, *47*, 8482. (c) Luisi, B. S.; Ma, Z.; Moulton, B. *J. Chem. Crystallogr.* **2007**, *37*, 743. (d) Vagin, S. I.; Ott, A. K.; Rieger, B. *Chem. Ing. Technol.* **2007**, *79*, 767. (e) Granifo, J.; Garland, M. T.; Baggio, R. *Polyhedron* **2006**, *25*, 2277. (f) Toh, N. L.; Nagarathinam, M.; Vittal, J. J. *Angew. Chem., Int. Ed.* **2005**, *44*, 2237. (g) Williams, C. A.; Blake, A. J.; Hubberstey, P.; Schröder, M. *Chem. Commun.* **2005**, 5435. (h) Mori, W.; Takamizawa, S.; Kato, C. N.; Ohmura, T.; Sato, T. *Microporous Mesoporous Mater.* **2004**, *73*, 31. (i) Yaghi, O. M.; O'Keeffe, M.; Ockwig, N. W.; Chae, H. K.; Eddaoudi, M.; Kim, J. *Nature* **2003**, *423*, 705. (j) Erxleben, A. *Coord. Chem. Rev.* **2003**, *246*, 203. (k) Ng, M. T.; Deivaraj, T. C.; Vittal, J. J. *Inorg. Chim. Acta* **2003**, *348*, 173. (l) Eddaoudi, M.; Moler, D. B.; Li, H.; Chen, B.; Reineke, T. M.; O'Keeffe, M.; Yaghi, O. M. *Acc. Chem. Res.* **2001**, *34*, 319. (m) Eddaoudi, M.; Li, H.; Reineke, T.; Fehr, M.; Kelley, D.; Groy, T. L.; Yaghi, O. M. *Top. Catal.* **1999**, *9*, 105.

(5) (a) Deeth, R. J. *Inorg. Chem.* **2008**, *47*, 6711. (b) Busskamp, H.; Deacon, G. B.; Hilder, M.; Junk, P. C.; Kynast, U. H.; Lee, W. W.; Turner, D. R. *Cryst. Eng. Comm.* **2007**, *9*, 394. (c) Cotton, F. A.; Wilkinson, G.; Murillo, C. A.; Bochmann, M. *Advanced Inorganic Chemistry*; 6th ed.; Wiley: New York, 1999; p 486. (d) Oldham, C. In *Comprehensive Coordination Chemistry*: Wilkinson, S. G.; Gillard, R. D.; McCleverty J. A., Eds.; Pergamon Press: London, 1987; Vol. *2*, p 435. (e) Mehrotra, R. C.; Bohra, R. *Metal Carboxylates*; Academic Press: New York, 1983. (f) Deacon, G. B.; Phillips, R. J. *Coord. Chem. Rev.* **1980**, *33*, 227.

Published on Web 12/03/2009

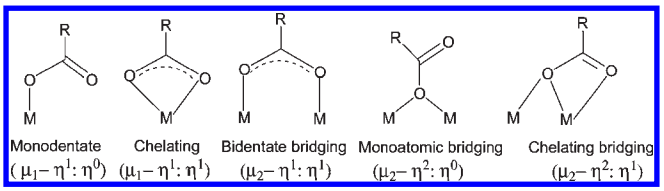

Figure 1. Various carboxylate coordination modes.

Lewis base coordinated zinc(II) carboxylate complexes in solution are labile partly because of a closed-shell d^{10} configuration and partly because of the ability of the carboxylate moiety to flip from one coordination mode to the other through a relatively less energetic "carboxylate shift" pathway illustrated in Figure 2. The carboxylate shift has important implications for metalloenzymes in understanding their catalytic activities.[6−9]

In the literature, Lewis base coordinated zinc(II) carboxylate complexes were prepared by (i) a condensation reaction involving zinc(II) carboxylate and the appropriate Lewis base[10−15] and (ii) a metathetical reaction involving zinc(II) salts with the salts of the corresponding carboxylic acid in the presence of a Lewis base.[16−20] The aforementioned routes were shown to afford a variety of discrete complexes with varying numbers of zinc as well as a coordination polymer depending upon the nature of the reactants, their ratio, Lewis base, and other reaction conditions. It was shown that subtle factors such as the nature of solvents used for crystallization and temperature also influence the nuclearity of the Lewis base coordinated zinc(II) acetate complexes.[10]

We wanted to understand the plausible mechanism of formation of Lewis base coordinated zinc(II) carboxylate complexes from their respective precursors in solution following the condensation route mentioned in the preceding paragraph, and hence $Zn(OAc)_2\cdot 2H_2O$ was treated with 3,5-lutidine (pK_a = 6.15), 2,3-lutidine (pK_a = 6.57), 2,4-lutidine (pK_a = 6.99), and 3,4-lutidine (pK_a = 6.46)[21] in a 1:1 molar ratio in methanol under identical reaction conditions. From these reactions, three discrete trinuclear complexes, namely, $[Zn_3(OAc)_2(\mu_2\text{-}\eta^2{:}\eta^1\text{-}OAc)_2(\mu_2\text{-}\eta^1{:}\eta^1\text{-}OAc)_2(H_2O)_2(3,5\text{-lutidine})_2]$ (**1**) and $[Zn_3(\mu_2\text{-}\eta^1{:}\eta^1\text{-}OAc)_4(\mu_2\text{-}\eta^2{:}\eta^0\text{-}OAc)_2L_2]$ [L = 2,3-lutidine (**2**) and 2,4-lutidine (**3**)], and a one-dimensional coordination polymer, $[Zn(OAc)(\mu_2\text{-}\eta^1{:}\eta^1\text{-}OAc)(3,4\text{-lutidine})]$ (**4**),[22] were isolated and structurally characterized. A plausible mechanism for the formation of complexes **1**−**4** is also presented.

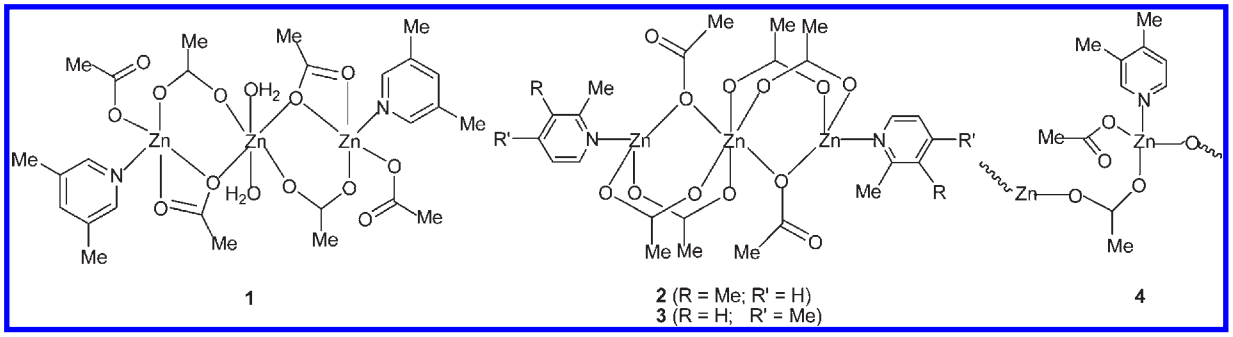

(6) (a) Sousa, S. F.; Fernandes, P. A.; Ramos, M. J. *J. Am. Chem. Soc.* **2007**, *129*, 1378. (b) Torrent, M.; Musaev, D. G.; Morokuma, K. *J. Phys. Chem. B* **2001**, *105*, 322.
(7) Rardin, R. L.; Tolman, W. B.; Lippard, S. J. *New. J. Chem.* **1991**, *15*, 417.
(8) Arnold, M.; Brown, D. A.; Degg, O.; Errington, W.; Haase, W.; Herlihy, K.; Kemp, T. J.; Nimir, H.; Werner, R. *Inorg. Chem.* **1998**, *37*, 2920.
(9) LeCloux, D. D.; Barrios, A. M.; Mizoguchi, T. J.; Lippard, S. J. *J. Am. Chem. Soc.* **1998**, *120*, 9001.
(10) Singh, B.; Long, J. R.; deBiani, F. F.; Gatteschi, D.; Stavropoulos, P. *J. Am. Chem. Soc.* **1997**, *119*, 7030.
(11) Clegg, W.; Little, I. R.; Straughan, B. P. *J. Chem. Soc., Dalton Trans.* **1986**, 1283.
(12) (a) Clegg, W.; Little, I. R.; Straughan, B. P. *Inorg. Chem.* **1988**, *27*, 1916. (b) Clegg, W.; Little, I. R.; Straughan, B. P. *J. Chem. Soc., Chem. Commun.* **1985**, 73.
(13) Attanasio, D.; Dessy, G.; Fares, V. *J. Chem. Soc., Dalton Trans.* **1979**, 28.
(14) Lalioti, N.; Raptopoulou, C. P.; Terzis, A.; Aliev, A. E.; Perlepes, S. P.; Gerothanassis, I. P.; Manessi-Zoupa, E. *Chem. Commun.* **1998**, 1513.
(15) Waheed, A.; Jones, R. A.; McCarty, J.; Yang, X. *Dalton Trans.* **2004**, 3840.
(16) Karmakar, A.; Sarma, R. J.; Baruah, J. B. *Inorg. Chem. Commun.* **2006**, *9*, 1169.
(17) (a) Baruah, A. M.; Karmakar, A.; Baruah, J. B. *Inorg. Chim. Acta* **2008**, *361*, 2777. (b) Karmakar, A.; Baruah, J. B. *Polyhedron* **2008**, *27*, 3409.
(18) Kwak, H.; Lee, S. H.; Kim, S. H.; Lee, Y. M.; Park, B. K.; Lee, E. Y.; Lee, Y. J.; Kim, C.; Kim, S.-J.; Kim, Y. *Polyhedron* **2008**, *27*, 3484.
(19) Zeleňák, V.; Sabo, M.; Massa, W.; Llewellyn, P. *Inorg. Chim. Acta* **2004**, *357*, 2049.
(20) Zeleňák, V.; Císařová, I.; Llewellyn, P. *Inorg. Chem. Commun.* **2007**, *10*, 27.

Experimental Section

Full experimental details pertinent to materials and methods can be found in the Supporting Information. Complexes **1**−**4** were prepared by a similar procedure, and a typical experimental procedure is described below for complex **1**. The reported yields of complexes **1**−**4** are based on $Zn(OAc)_2\cdot 2H_2O$.

$[Zn_3(OAc)_2(\mu_2\text{-}\eta^2{:}\eta^1\text{-}OAc)_2(\mu_2\text{-}\eta^1{:}\eta^1\text{-}OAc)_2(H_2O)_2(3,5\text{-lutidine})_2]$ (1). $Zn(OAc)_2\cdot 2H_2O$ (500 mg, 2.28 mmol) was dissolved in methanol (20 mL). To the aforementioned solution was added 3,5-lutidine (250 mg, 2.33 mmol) in methanol (5 mL). The homogeneous mixture was stirred at room temperature for 12 h, concentrated under a vacuum to ~5 mL, and the solution left at room temperature to afford colorless crystals. Crystals were separated and washed with cold *n*-hexane to afford complex **1** in 93% yield (570 mg, 0.71 mmol). Crystals suitable for X-ray diffraction data were obtained from methanol at room temperature over the period of a week. FT-IR data (KBr, cm^{-1}): 3402 (br) for $\nu(H_2O)$; 1601 (br, vs), 1577 (sh), 1571 (sh) for $\nu_{asym}(OCO)$; and 1421 (br, s), 1396 (sh) for $\nu_{sym}(OCO)$. ^1H NMR ($CDCl_3$, 300 MHz, δ ppm): 2.07 (s, 18H, $OC(O)CH_3$), 2.37 (s, 12H, $NC_5H_3(CH_3)_2$-3,5), 2.95 (s, 4H, H_2O), 7.55 (s, 2H,

(21) *CRC Handbook of Chemistry and Physics*, 81st ed.; Lide, D. R., Ed.; CRC Press: New York, 2000/2001; Section 8.
(22) We prefer not to use *n* or ∞ in representing coordination polymer **4**. This issue was discussed in detail in the following reference: Biradha, K.; Ramanan, A.; Vittal, J. J. *Cryst. Growth Des.* **2009**, *9*, 2969.

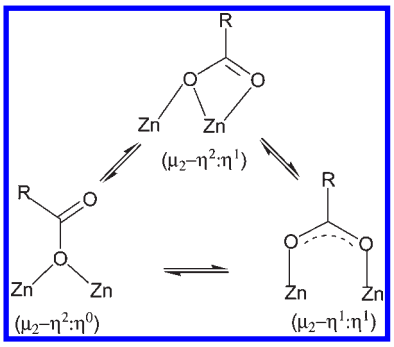

Figure 2. "Carboxylate shift" process.

4*H* $NC_5H_3(CH_3)_2$-3,5, 8.33 (s, 4H, 2*H* & 6*H* $NC_5H_3(CH_3)_2$-3,5). ^{13}C NMR ($CDCl_3$, 75.5 MHz, δ ppm): 18.0, 22.4 (*C*H_3), 134.4, 140.5, 146.3 (N*C*$_5H_3(CH_3)_2$-3,5), 179.7 (O*C*(O)CH_3). Solid-state CPMAS ^{13}C NMR (75.5 MHz, δ ppm): 17.7, 19.0, 22.1, 24.2 (*C*H_3), 133.6, 141.0, 145.7 (N*C*$_5H_3(CH_3)_2$-3,5), 177.2, 180.3 (O*C*(O)CH_3). MS (TOF, ES$^+$): *m*/*z* 801 $[M]^+$ (11%), 587 $[L_2Zn_2(OAc)_4 + Li]^+$ (18%), 560 $[LZn_2(OAc)_4(H_2O) + Na + K]^+$ (13%), 456 $[L_2Zn(OAc)_2(H_2O)_2 + Na]^+$ (19%), 418 $[L_2Zn(OAc)_2(H_2O)]^+$ (36%), 388 $[LZn(OAc)_2(H_2O)_2 + Na + K]^+$ (38%), 342 $[LZn(OAc)_2(H_2O)_2 + 2\ Li]^+$ (42%), 271 $[Zn(OAc)_2(H_2O)_2 + K + 2\ Li]^+$ (26%), 242 $[Zn(OAc)_2(H_2O)_2 + Na]^+$ (100%). Anal. Calcd for $C_{26}H_{40}N_2O_{14}Zn_3$: C, 39.00; H, 5.03; N, 3.50. Found: C, 38.79; H, 5.01; N, 3.46%.

[$Zn_3(\mu_2$-η^1:η^1-OAc)$_4(\mu_2$-η^2:η^0-OAc)$_2$(2,3-lutidine)$_2$] (2). Yield: 79% (460 mg, 0.60 mmol). FT-IR data (KBr, cm^{-1}): 1637 (s), 1597 (vs) for ν_{asym}(OCO); 1436 (vs), 1408 (s), and 1390 (sh) for ν_{sym}(OCO). ^{1}H NMR ($CDCl_3$, 300 MHz, δ ppm): 2.11 (s, 18H, OC(O)C*H*$_3$), 2.36, 2.59 (each s, 12H, $NC_5H_3(CH_3)_2$−2,3), 7.24 (t, 2H, 5*H* $NC_5H_3(CH_3)_2$-2,3, J_{HH} = 6.3 Hz), 7.63 (d, 2H, 4*H* $NC_5H_3(CH_3)_2$-2,3, J_{HH} = 7.5 Hz), 8.46 (d, 2H, 6*H* $NC_5H_3(CH_3)_2$-2,3, J_{HH} = 5.1 Hz). ^{13}C NMR ($CDCl_3$, 75.5 MHz, δ ppm): 19.4, 21.8, 23.0 (*C*H_3), 122.2, 133.5, 139.8, 146.3, 157.4 (N*C*$_5H_3(CH_3)_2$-2,3), 180.4 (O*C*(O)CH_3). Solid-state CPMAS ^{13}C NMR data (75.5 MHz, δ ppm): 18.4, 20.7, 22.2, 23.8, 24.3 (*C*H_3), 122.9, 133.3, 141.6, 145.9, 157.4 (N*C*$_5H_3(CH_3)_2$-2,3), 176.6, 178.4 (O*C*(O)CH_3). MS (TOF, ES$^+$): *m*/*z* 765 $[M]^+$ (4%), 609 $[L_2Zn_2(OAc)_4 + Na + Li]^+$ (3%), 532 $[LZn_2(OAc)_4(H_2O) + K]^+$ (9%), 455 $[L_2Zn(OAc)_2(H_2O)_2 + Na]^+$ (11%), 360 $[LZn(OAc)_2(H_2O) + K + 2\ Li]^+$ (22%), 317 $[LZn(OAc)_2(H_2O) + 2\ Li]^+$ (100%). Anal. Calcd for $C_{26}H_{36}N_2O_{12}Zn_3$: C, 40.83; H, 4.74; N, 3.66. Found: C, 40.61; H, 4.76; N, 3.42%. Crystals suitable for X-ray diffraction data were grown from a methanol/diethyl ether mixture at room temperature over two days.

[$Zn_3(\mu_2$-η^1:η^1-OAc)$_4(\mu_2$-η^2:η^0-OAc)$_2$(2,4-lutidine)$_2$] (3). Yield: 81% (470 mg, 0.61 mmol). FT-IR data (KBr, cm^{-1}): 1636 (vs), 1624 (vs) for ν_{asym}(OCO); 1421 (s) for ν_{sym}(OCO). ^{1}H NMR ($CDCl_3$, 300 MHz, δ ppm): 2.10 (s, 18H, OC(O)C*H*$_3$), 2.40, 2.61 (each s, 12H, $NC_5H_3(CH_3)_2$-2,4), 7.12 (d, 2H, 5*H* $NC_5H_3(CH_3)_2$-2,4, J_{HH} = 5.4 Hz), 7.15 (s, 2H, 3*H* $NC_5H_3(CH_3)_2$-2,4), 8.45 (d, 2H, 6*H* $NC_5H_3(CH_3)_2$-2,4, J_{HH} = 5.4 Hz). ^{13}C NMR ($CDCl_3$, 75.5 MHz, δ ppm): 21.0, 22.8, 23.2 (*C*H_3), 122.9, 126.1, 148.2, 151.5, 158.0 (N*C*$_5H_3(CH_3)_2$-2,4), 180.0 (O*C*(O)CH_3). Solid-state CPMAS ^{13}C NMR (75.5 MHz, δ ppm): 21.0, 23.5 (*C*H_3), 124.3, 127.5, 147.6, 153.6, 158.7 (N*C*$_5H_3(CH_3)_2$-2,4), 177.5, 178.6 (O*C*(O)CH_3). MS (TOF, ES$^+$): *m*/*z* 764 $[M]^+$ (27%), 451 $[L_2Zn(OAc)_2(H_2O)_3]^+$ (31%), 410 $[LZn(OAc)_2(H_2O)_2 + 2K + Li]^+$ (15%), 317 $[LZn(OAc)_2(H_2O) + Li]^+$ (10%), 275 $[Zn(OAc)_2(H_2O)_3 + Na + 2\ Li]^+$ (57%), 243 $[Zn(OAc)_2(H_2O)_2 + Na]^+$ (44%), 215 $[Zn(OAc)_2 + Na + Li]^+$ (48%). Anal. Calcd for $C_{26}H_{36}N_2O_{12}Zn_3$: C, 40.83; H, 4.74; N, 3.66. Found: C, 40.50; H, 4.78; N, 3.61%. Crystals suitable for X-ray diffraction data were grown from a methanol/diethyl ether mixture at room temperature over two days.

[Zn(OAc)(μ_2-η^1:η^1-OAc)(3,4-lutidine)] (4). Yield: 94% (620 mg, 2.14 mmol). FT-IR data (KBr, cm^{-1}): 1571 (s), 1557 (sh) for ν_{asym}(OCO); 1414 (sh), 1395 (vs) for ν_{sym}(OCO). ^{1}H NMR ($CDCl_3$, 300 MHz, δ ppm): 2.06 (s, 6H, OC(O)C*H*$_3$), 2.30, 2.34 (each s, 6H, $NC_5H_3(CH_3)_2$-3,4), 7.24 (d, 1H, 5*H* $NC_5H_3(CH_3)_2$-3,4, J_{HH} = 5.4 Hz), 8.43 (d, 1H, 6*H* $NC_5H_3(CH_3)_2$-3,4, J_{HH} = 4.8 Hz), 8.44 (s, 1H, 2*H* $NC_5H_3(CH_3)_2$-3,4). ^{13}C NMR ($CDCl_3$, 75.5 MHz, δ ppm): 16.4, 19.3, 22.6 (*C*H_3), 125.7, 134.0, 146.5, 148.7, 150.2 (N*C*$_5H_3(CH_3)_2$-3,4), 179.9 (O*C*(O)CH_3). Solid-state CPMAS ^{13}C NMR (75.5 MHz, δ ppm): 15.9, 22.5 (*C*H_3), 126.0, 133.8, 146.1, 150.3, 152.1 (N*C*$_5H_3(CH_3)_2$-3,4), 177.3, 183.0 (O*C*(O)CH_3). Anal. Calcd for $C_{11}H_{15}NO_4Zn$: C, 45.46; H, 5.20; N, 4.82. Found: C, 45.26; H, 5.11; N, 4.78%. Crystals suitable for X-ray diffraction data were grown by diffusing *n*-hexane over a CH_2Cl_2 solution of **4** at room temperature over two days.

The reaction of $Zn(OAc)_2\cdot 2H_2O$ (500 mg, 2.28 mmol) with 2,6-lutidine (250 mg, 2.33 mmol) in methanol (25 mL) under conditions identical to those mentioned for complex **1** afforded no new product, as revealed by ^{1}H NMR spectroscopy.

Crystal Structure Determination. X-ray diffraction studies of suitably sized crystals mounted on a capillary were carried out on a BRUKER AXS SMART-APEX diffractometer with a CCD area detector (Mo Kα, 0.71073 Å, graphite monochromator).[23] Frames were collected at 298 K by ω, ϕ, and 2θ rotation at 10 s per frame with SMART.[23] The measured intensities were reduced to F^2 and corrected for absorption with SADABS.[24] Structure solution, refinement, and data output were carried out with the SHELXTL program.[25] Non-hydrogen atoms were refined anisotropically. C−H hydrogen atoms were placed in geometrically calculated positions by using a riding model. O−H hydrogen atoms were located in a difference Fourier map and refined isotropically by fixing the observed position in subsequent refinement cycles. Images were created with the Diamond program.[26] Hydrogen-bonding interactions in the crystal lattice were calculated with SHELXTL.[25] The X-ray crystallographic parameters, details of data collection, and structure refinement are presented in Table 1.

Results and Discussion

$Zn(OAc)_2\cdot 2H_2O$ was treated with 3,5-lutidine, 2,3-lutidine, 2,4-lutidine, and 3,4-lutidine in a 1:1 molar ratio in methanol under identical conditions to obtain the lutidine coordinated zinc(II)acetate complexes and to understand the plausible mechanism of formation of the products. Further, the structural information obtained for the products was anticipated to shed light on the "carboxylate shift" concept. From the aforementioned reactions, three discrete trinuclear complexes **1**−**3** and a one-dimensional coordination polymer **4** were isolated in 93, 79, 81, and 94% yields, respectively.

Crystal and Molecular Structures of Complexes 1−4. The molecular structures of complexes **1**−**4** were determined by single-crystal X-ray diffraction data. The ORTEP representations of complexes **1**−**4** with the atom labeling scheme are shown in Figures 3−6, respectively. Selected bond parameters for complexes **1**−**4** are listed in Tables 2−4. Complex **1** consists of a linear trinuclear Zn(II) unit with the central Zn(II) residing on a crystallographic inversion center and is coordinated to the

(23) *SMART: Bruker Molecular Analysis Research Tool*, version 5.0; Bruker Analytical X-ray Systems: Madison, WI, 2000.
(24) *SAINT-NT*, version 6.04; Bruker Analytical X-ray Systems: Madison, WI, 2001.
(25) Sheldrick, G. M. *SHELXTL-NT, Version 6.12, Reference Manual*; Bruker-AXS: Madison, WI.
(26) Klaus, B. *DIAMOND*, version 3.0 c; University of Bonn: Bonn, Germany, 2004.

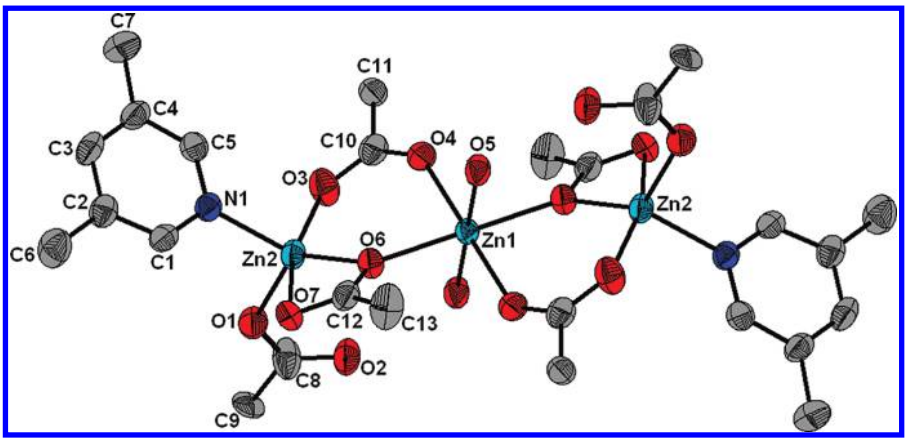

Figure 3. An ORTEP representation of complex **1** at the 50% probability level. Hydrogen atoms omitted for clarity.

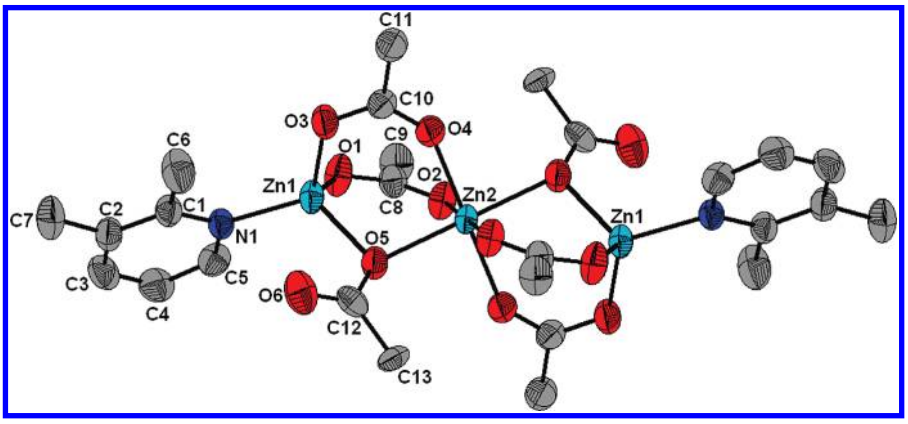

Figure 4. An ORTEP representation of complex **2** at the 50% probability level. Hydrogen atoms omitted for clarity.

Table 1. Crystallographic and Experimental Data for Complexes **1**−**4**

	1	**2**	**3**	**4**
formula	$C_{26}H_{40}N_2O_{14}Zn_3$	$C_{26}H_{36}N_2O_{12}Zn_3$	$C_{26}H_{36}N_2O_{12}Zn_3$	$C_{11}H_{15}NO_4Zn$
fw	800.77	764.74	764.74	290.64
cryst syst	triclinic	triclinic	triclinic	monoclinic
space group	$P\bar{1}$	$P\bar{1}$	$P\bar{1}$	$P2_1/c$
a (Å)	8.037(2)	7.677(4)	8.114(6)	7.9956(11)
b (Å)	8.072(2)	10.114(6)	8.595(7)	8.4047(12)
c (Å)	14.774(4)	11.599(6)	2.566(10)	19.580(3)
α (deg)	97.196(5)	69.651(9)	109.914(8)	90.00
β (deg)	95.077(5)	74.983(8)	97.534(2)	99.392(3)
γ (deg)	116.266(4)	72.430(9)	96.222(5)	90.00
vol (Å^3)	838.6(4)	749.3(8)	804.7(11)	1298.6(3)
Z	1	1	1	4
density (calcd), g cm^{-3}	1.586	1.599	1.578	1.487
T (K)	298(2)	298(2)	298(2)	298(2)
λ(Mo Kα) (Å)	0.71073	0.71073	0.71073	0.71073
μ(Mo Kα) (cm^{-1})	2.194	2.308	2.278	1.893
R_1, $R_{W2}[I > 2\sigma(I)]^a$	0.0374, 0.0870	0.0400, 0.1404	0.0629, 0.1283	0.0581, 0.1398
R_1, R_{W2} (all data)^a	0.0443, 0.0838	0.0574, 0.1207	0.0779, 0.1350	0.0668, 0.1447

^{a} $R_1 = \sum||F_o| - |F_c||/\sum|F_o|$; $wR_2 = [\sum w(|F_o| - |F_c|)^2/\sum w|F_o|^2]^{1/2}$.

adjacent pair of centrosymmetrically related Zn(II) by syn−syn bidentate bridging and asymmetric chelating bridging acetate moieties. The remaining two coordination sites on the central Zn(II) are occupied by two water molecules to afford an octahedral geometry, whereas those on the terminal Zn(II) are occupied by a monodentate acetate and a 3,5-lutidine, affording a severely distorted trigonal bipyramidal geometry. The Zn2−O7, 2.483(2) Å, distance is significantly longer than the remaining Zn−O bonds around the terminal zincs that vary over 1.946(2)−2.012(2) Å. Further, the C(12)−O(7), 1.229(3) Å, distance is shorter than the C(12)−O(6), 1.296(3) Å, distance, indicating an asymmetric chelating bridging acetate coordination mode. The metrical parameters around the terminal zincs in **1** compare well with one of the terminal zincs in the MOF {[Zn_3(1,4-BDC)$_3$-(DEF)$_2$]·DEF} (1,4-BDC = 1,4−benzene dicarboxylate; DEF = diethylformamide).[4g] Complex **1** is unique in that

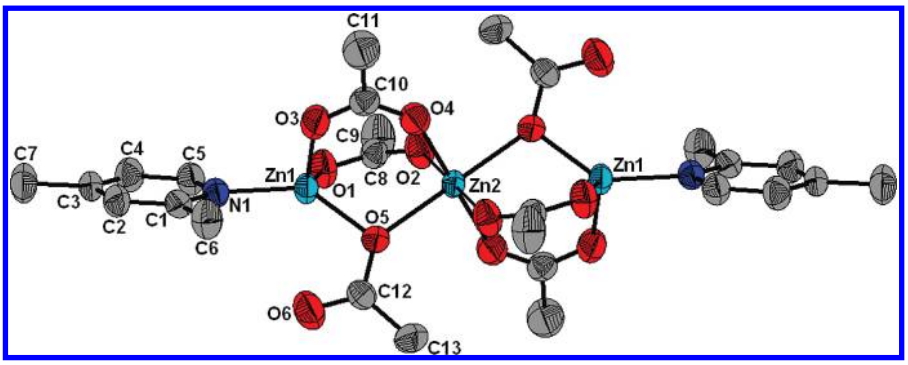

Figure 5. An ORTEP representation of complex **3** at the 50% probability level. Hydrogen atoms omitted for clarity.

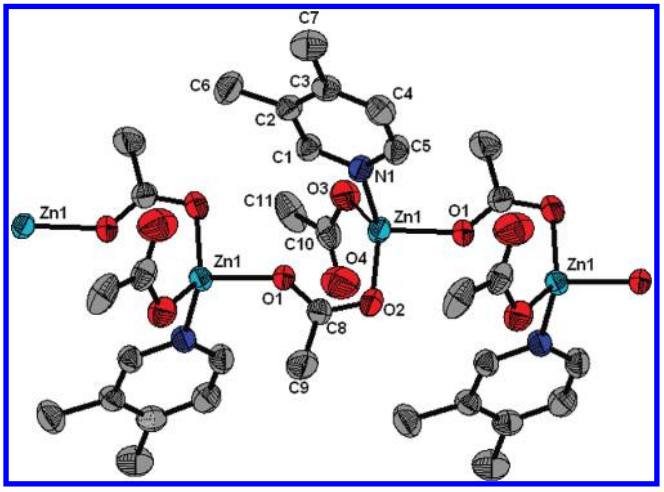

Figure 6. View of the 1D helical chain of complex **4** at the 50% probability level running along the *b* axis. Hydrogen atoms omitted for clarity.

Table 2. Selected Bond Lengths (Å) and Bond Angles (deg) for Complex **1**

Zn1−O4	2.065(2)	Zn2−O3	1.976(2)
Zn1−O5	2.094(2)	Zn2−O6	2.012(2)
Zn1−O6	2.180(2)	Zn2−O7	2.483(2)
Zn2−O1	1.946(2)	Zn2−N1	2.076(2)
O4−Zn1−O5	90.80(8)	O3−Zn2−N1	96.93(9)
O4−Zn1−O6	92.13(7)	O6−Zn2−N1	120.99(8)
O5−Zn1−O6	92.00(7)	O7−Zn2−N1	87.50(8)
O6−Zn1−O6′	180.00(1)	O1−Zn2−O7	96.34(9)
O1−Zn2−O3	106.3(1)	O3−Zn2−O7	155.86(8)
O1- Zn2−O6	127.42(8)	O6−Zn2−O7	56.74(7)
O3−Zn2−O6	101.58(8)	N1−Zn2−O7	87.50(8)
O1−Zn2−N1	98.88(8)		

Table 3. Selected Bond Lengths (Å) and Bond Angles (deg) for Complexes **2** and **3**

	2	**3**		**2**	**3**
Zn1−O1	1.961(3)	1.958(3)	Zn2−O2	2.070(3)	2.085(3)
Zn1−O3	1.940(3)	1.953(3)	Zn2−O4	2.110(3)	2.045(3)
Zn1−O5	1.980(3)	1.962(3)	Zn2−O5	2.156(2)	2.152(3)
Zn1−N1	2.025(3)	2.026(4)			
O3−Zn1−O1	107.4(1)	115.2(1)	O2−Zn2−O4	92.8(1)	86.3(1)
O3−Zn1−O5	109.2(1)	102.8(1)	O2−Zn2−O4′	87.2(1)	93.7(1)
O1−Zn1−O5	102.1(1)	100.8(1)	O4−Zn2−O4	180.00(1)	180.0(1)
O3−Zn1−N1	118.8(1)	100.0(2)	O2−Zn2−O5	89.9(1)	90.4(1)
O1−Zn1−N1	97.7(1)	98.6(1)	O2−Zn2−O5′	90.1(1)	89.6(1)
O5−Zn1−N1	118.7(1)	140.0(1)	O4−Zn2−O5	89.8(1)	89.8(1)
O2−Zn2−O2	180.00(1)	180.00(1)			

it contains three types of acetate coordination modes, namely, monodentate, bridging bidentate, and asymmetric chelating bridging. We are aware that

Table 4. Selected Bond Lengths (Å) and Bond Angles (deg) for Complex **4**

Zn1−N1	2.052(3)	Zn1−O2	1.994(3)
Zn1−O1	1.971(2)	Zn1−O3	1.941(3)
N1−Zn1−O1	105.8(1)	O3−Zn1−O2	135.7(1)
N1−Zn1−O3	98.7(1)	O2−Zn1−O1	95.2(1)

Table 5. Significant Hydrogen Bond Parameters (Interatomic Distances in Å and Bond Angles in deg) found in the Crystal Lattice of Complex **1**

D−H···A	D−H	H···A	D···A	D−H···A
O5−H5C···O2	0.82	1.98	2.73	152
O5−H5B···O2[a]	0.82	2.04	2.83	162
C6−H6B···O7	0.96	2.64	3.59	170
C3−H3···O1	0.93	2.72	3.52	145

[a] Symmetry code: $1-x, 1-y, 1-z$.

$(Me_4N)[Nb_2Cl_2(tht)(\mu_2\text{-}\eta^2\text{:}\eta^1\text{-OAc})(\mu_1\text{-}\eta^1\text{:}\eta^1\text{-OAc})_2(\mu_2\text{-}\eta^1\text{:}\eta^1\text{-OAc})_2]$ (tht = tetrahydrothiophene) is the only other complex known to possess three different acetate coordination modes.[27]

Significant hydrogen-bond parameters observed in complex **1** are listed in Table 5. Two water molecules on the central Zn(II) in **1** act as a hydrogen-bond donor to the carbonyl oxygen of the monodentate acetate within the molecule (intramolecular hydrogen bonding) and the carbonyl oxygen of the monodentate acetate in the inversion related adjacent molecule (intermolecular hydrogen bonding) and thus form an eight-membered ring (R_4^2 (8), Figure 7).[28] In addition, the O7 atom of the asymmetric chelating bridging acetate is involved in C−H···O hydrogen bonding with one of the hydrogen atoms bonded to C6 while O1 of monodentate acetate is involved in the second C−H···O hydrogen bond with the *p*-hydrogen of the 3,5-lutidine in the inversion related adjacent molecule. The aforementioned hydrogen-bonding network grows along the *bc* plane to afford a two-dimensional sheet, as depicted in Figure 7. The two-dimensional sheet is further strengthened by an offset π-stacking interaction between 3,5-lutidine in the reference molecule and that in the inversion related adjacent molecule with a centroid-to-centroid distance of 3.54 Å. The centroid-to-centroid distance in **1** is in a range anticipated for the $\pi\cdots\pi$ distance between pyridine-type aromatics (3.4−3.8 Å).[29] We believe that the noncovalent interactions in the crystal

(27) Cotton, F. A.; Diebold, M. P.; Matusz, M.; Roth, W. J. *Inorg. Chim. Acta* **1986**, *112*, 147.
(28) Bernstein, J.; Davis, R. E.; Shimoni, L.; Chang, N.-L. *Angew. Chem., Int. Ed. Engl.* **1995**, *34*, 1555.
(29) Janiak, C. *J. Chem. Soc., Dalton Trans.* **2000**, 3885.

lattice could have stabilized complex **1** in the shown framework.

Complexes **2** and **3** possess a cage framework, and this framework resembles that reported for $[Zn_3(\mu_2\text{-}\eta^1\text{:}\eta^1\text{-}O_2CR)_4(\mu_2\text{-}\eta^2\text{:}\eta^0\text{-}O_2CR)_2L_2]$ [R/L: Me/py (**I**),[10] MeCH=CH/quinoline (**II**),[12b] and Ph/nicotinamide (**III**)[19]].

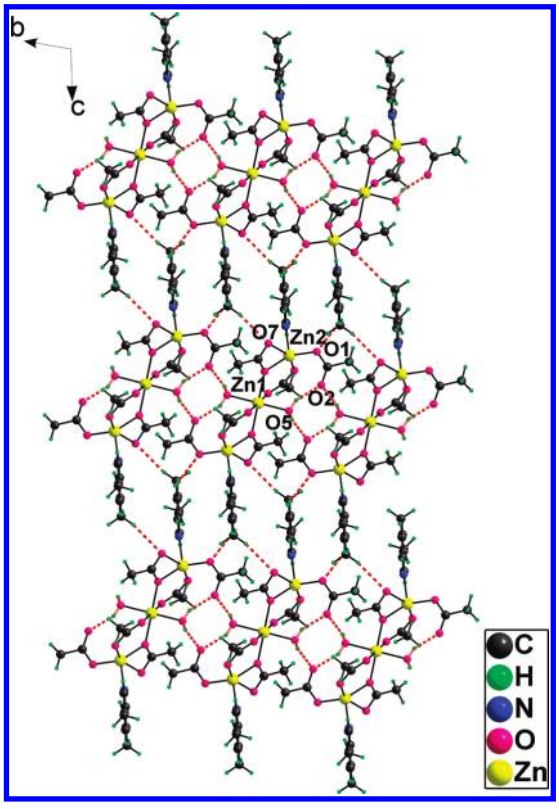

Figure 7. Packing diagram showing both O−H···O and C−H···O hydrogen bonding in complex **1**.

The values of metrical parameters *A*, *B*, *D*, α, *β*, *γ*, and *θ* associated with the geometry of a monoatomic bridging acetate in trinuclear complexes **1**−**3** and **I**−**III** are listed in Table 6 to gain insight concerning the "carboxylate shift" concept.[7] The values of *A* and *B* in complex **1** are slightly longer than those observed in **I**, **2**, and **3**. The value of *D* is significantly shorter, but the value of Zn···Zn is significantly longer in **1** than those observed in **I**, **2**, and **3**. Complex **1** differs from complexes **I**, **2**, and **3** in that it only contains one bidentate bridging acetate whereas complexes **I**, **2**, and **3** each contain two. Thus, the observed variations in Zn···Zn separation and *D* may be the result of the second bridging acetate versus the basicity/sterics of the Lewis base. The values of *γ* and *θ* are higher, but the value of *β* is smaller in complex **1** than those found in **I**, **2**, and **3**. These structural features suggest that either less basic L or more basic and more sterically hindered L shifts the acetate coordination mode from asymmetric chelating bridging to monoatomic bridging (see Figure 2).

No meaningful trend concerning the "carboxylate shift" concept emerged upon comparison of the structural parameters of **I** with those of **II** and **III**, perhaps owing to the complexity associated with subtle electronic/steric properties of the Lewis bases and the carboxylate moieties as well as noncovalent interactions in the crystal lattice. In fact, complex **I** is devoid of noncovalent interactions, whereas **II** and **III** are shown to possess intermolecular C−H···O/*π*···*π* and N−H···O/C−H···O interactions, respectively, in the crystal lattice.

Lippard and co-workers compared the values of the parameters indicated in Table 6 for the structurally analogous Lewis base coordinated diiron tetracarboxylate complexes and concluded that changing either the steric bulk of the carboxylate subsituent or the basicity of the Lewis base shifted the carboxylate coordination mode

Table 6. Comparison of Metrical Parameters Associated with Monoatomic Bridging Acetate in Complexes **1**−**3** and **I**−**III** (Interatomic Distances in Å and Bond Angles in deg)

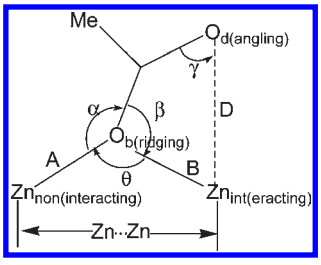

	1	2	3	I	II	III
A	2.180(2)	2.155 (2)	2.152(3)	2.130(3)	2.177(2)	2.201(1)
B	2.012(2)	1.980(3)	1.962(3)	1.951(3)	1.954(2)	1.996(1)
D	2.482(2)	2.793(2)	2.790(2)	2.781(3)	2.752 (3)	2.780(1)
Zn···Zn	3.626(1)	3.280(2)	3.290(2)	3.233(1)	3.264(2)	3.1845(2)
C−O_b	1.296(3)	1.303(4)	1.290(5)	1.289(5)	1.306(3)	1.306(3)
C−O_d	1.229(3)	1.209 (5)	1.220(5)	1.211(5)	1.219(3)	1.228(2)
O_b−C−O_d	118.9(3)	121.3(4)	120.1(4)	121.2(4)	120.8(3)	121.1 (2)
α	137.8(1)	133.3(2)	139.8(3)	137.2(2)	133.8(2)	126.4 (1)
β	102.2(1)	112.0(2)	113.6(3)	112.8(2)	111.4(2)	109.4(1)
γ	82.0(2)	75.3(3)	75.3(3)	74.7(2)	75.5(1)	74.7(1)
τ = α − *β*	35.6	21.3	26.2	24.4	22.4	17.0
θ	119.8(1)	104.9(1)	106.1(1)	104.7(1)	104.2(1)	98.6 (1)
N−Zn−O_b	121.0(1)	118.8 (1)	140.0(1)	130.7(1)	130.4 (1)	118.8(1)

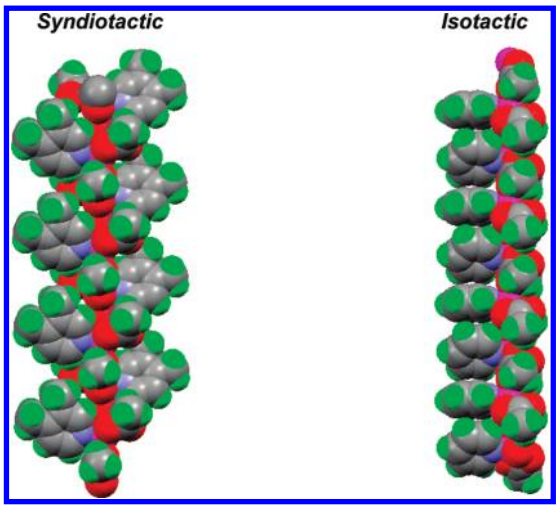

Figure 8. Space fill models for complexes **4** (left) and **IV** (right).

from monoatomic bridging to syn−syn bidentate bridging.[9] Further, the Lewis base coordinated metal carboxylates were classified into three classes depending upon the values of the parameters listed in Table 6.[7] According to this classification, complexes **2** and **3** belong to class I, whereas complex **1** belongs to the first structurally characterized class II zinc(II) carboxylate complex. Both complexes **2** and **3** are stabilized by C−H···O hydrogen-bonding interactions in the crystal lattice (see the Supporting Information).

In complex **4**, the Zn(II) is tetrahedrally surrounded by a 3,4-lutidine, O(3) of the monodentate acetate, O(2) of the syn−anti bridging acetate, and O(1) of the syn−anti bridging acetate from the next repeating unit of the polymer related by a screw axis $(1 - x, 1/2 + y, 1/2 - z$; see Figure 6). In the related [Zn(μ_1-η^1:η^1-OAc)(μ_2-η^1:η^1-OAc)py] (**IV**),[10] the Zn(II) is surrounded by a pyridine, two syn−anti bridging acetates, and an asymmetric chelating acetate and is thus five-coordinated. The nonbonded Zn···Zn separations within the repeating unit and between the repeating units in **IV** are 4.687 and 4.552 Å, and these distances are longer than that observed for complex **4** (4.415(1) Å). Another notable difference between **4** and **IV** is that the 3,4-lutidine in complex **4** is situated on the opposite side of the growing polymer and thus renders a *syndiotactic* stereochemistry, whereas pyridine is placed on the same side of the growing polymer giving an *isotactic* arrangement for **IV**, as shown in Figure 8. We believe that the aforementioned structural differences arise due to the difference in the steric and basic properties of Lewis bases. The topology of the polymer in **4** resembles that reported for [Zn(cinn)$_2$(mpcm)] (cinn = cinnamato, mpcm = methyl-3-pyridylcarbamate) (**V**).[20] However, the nonbonded Zn···Zn separation, 4.415(1) Å, and Zn−O$_d$ distance, 2.729(4) Å, in **4** are shorter than those reported for **V** [4.7750(3) and 3.141(2) Å, respectively].[20] Complex **4** is stabilized by C−H···O hydrogen bonding in the crystal lattice (see the Supporting Information). The nuclearity/aggregation and acetate coordination modes in complexes **1**−**4** thus appear to depend upon the subtle basic/steric properties of lutidine versus noncovalent interactions formed during the synthesis of the products.

Spectroscopic Properties of Complexes 1−4. IR spectroscopy is one of the useful techniques used to assign the carboxylate coordination modes, and the following trend is generally accepted as a guideline to differentiate various carboxylate coordination modes.[5e,f,30]

$$\Delta\nu = \nu_{asym}(OCO) - \nu_{sym}(OCO)$$

$$\Delta\nu \text{ chelating} < \Delta\nu \text{ bridging} < \Delta\nu \text{ ionic} < \Delta\nu \text{ monodentate}$$

More precisely, comparison of the $\Delta\nu$ value of the respective carboxylate complexes with the $\Delta\nu$ value of the sodium salt of the same carboxylate should be used as a guideline in assigning the carboxylate coordination modes. Accordingly, (i) the chelating coordination mode occurs when $\Delta\nu$ of the studied complex $\ll \Delta\nu$ of the sodium salt; (ii) the bidentate bridging coordination mode occurs when $\Delta\nu$ of the studied complex $\leq \Delta\nu$ of the sodium salt, and (iii) the monodentate coordination mode exists when $\Delta\nu$ of the studied complex $\gg \Delta\nu$ of the sodium salt.[5e,f,30]

The IR spectrum of complex **1** revealed an intense broad band at 3402 cm^{-1}, indicating the presence of coordinated water molecules in the crystal lattice. Further, complex **1** revealed an intense band at 1601 cm^{-1} with two shoulders at 1577 and 1571 cm^{-1} for ν_{asym}(OCO) and an intense band at 1421 cm^{-1} with a shoulder at 1396 cm^{-1} for ν_{sym}(OCO). The $\Delta\nu$ = 205 cm^{-1} value of complex **1** is higher than that reported for sodium acetate ($\Delta\nu$ = 164 cm^{-1})[31] and thus indicates a monodentate acetate coordination mode, and we assign the $\Delta\nu$ = 175 cm^{-1} value for syn−syn bidentate bridging and the $\Delta\nu$ = 156 cm^{-1} value for asymmetric chelating bridging. Complex **2** revealed two bands at 1637 and 1597 cm^{-1} assignable for ν_{asym}(OCO) and three bands at 1436, 1408, and 1390 cm^{-1} assignable for ν_{sym}(OCO), whereas complex **3** revealed two bands at 1636 and 1624 cm^{-1} assignable for ν_{asym}(OCO) and a band at 1421 cm^{-1} assignable for ν_{sym}(OCO). Thus, the $\Delta\nu$ = 189 and 161 cm^{-1} values for complex **2** and $\Delta\nu$ = 215 cm^{-1} value for complex **3** correspond to syn−syn bidentate bridging, whereas the $\Delta\nu$ = 247 cm^{-1} value for complex **2** and $\Delta\nu$ = 203 cm^{-1} value for complex **3** correspond to monoatomic bridging. The IR spectrum of complex **4** revealed two bands at 1571 and 1557 cm^{-1} assignable to ν_{asym}(OCO) and two bands at 1414 and 1395 cm^{-1} assignable to ν_{sym}(OCO). The $\Delta\nu$ = 176 cm^{-1} value for the first pair indicates a monodentate acetate coordination mode, and the $\Delta\nu$ = 143 cm^{-1} value for the second pair indicates a syn−anti bidentate bridging coordination mode.

Tasumi et al. suggested an empirical equation (eq 1) that relates $\Delta\nu_{calcd}$ with metrical parameters δr and θoco obtained from single-crystal X-ray diffraction data:[32]

$$\Delta\nu_{calcd} = 1818.1\delta r + 16.47(\theta oco - 120) + 66.8... \quad (1)$$

(30) (a) Zeleňák, V.; Vargová, Z.; Györyová, K. *Spectrochim. Acta, Part A* **2007**, *66*, 262. (b) Nakamoto, K. *Infra-red and Raman Spectra of Inorganic and Coordination Compounds*, 5th ed.; Wiley: New York, 1997.
(31) Ito, K.; Bernstein, H. J. *Can. J. Chem.* **1956**, *34*, 170.
(32) Nara, M.; Torii, H.; Tasumi, M. *J. Phys. Chem.* **1996**, *100*, 19812.

Table 7. $\Delta\nu_{calcd}$ and $\Delta\nu_{exp}$ Values and Coordination Modes in Complexes **1**−**4**

	$\Delta\nu_{calcd}$ ($\Delta\nu_{exp}$) (cm^{-1})	coordination mode
1	204 (205)	monodentate
	170 (156)	asymmetric chelating bridging
	177 (175)	syn−syn bidentate bridging
2	204 (189), 196 (161)	syn−syn bidentate bridging
	259 (247)	monoatomic bridging
3	220 (215)	syn−syn bidentate bridging
	196 (203)	monoatomic bridging
4	105 (143)	syn−anti bidentate bridging
	173 (176)	monodentate

where δr is the difference between the two C−O bond lengths (in ångstroms) and θoco is the OCO angle (in degrees). Ishioka et al. applied eq 1 to anhydrous Zn(OAc)$_2$ and Zn(OAc)$_2\cdot$2H$_2$O,[33] and subsequently Zeleňák et al. applied eq 1 to several Lewis base coordinated zinc(II) carboxylates bearing distinct carboxylate coordination modes to better interpret $\Delta\nu$ values in these compounds.[30a] In Table 7, we compared the values of $\Delta\nu_{calcd}$ obtained from eq 1 with $\Delta\nu_{exp}$ obtained from the IR spectra of complexes **1**−**4**. There is fairly good agreement between the $\Delta\nu_{calcd}$ and $\Delta\nu_{exp}$ values for the monodentate acetate coordination mode in complexes **1** and **4**, the asymmetric chelating bridging mode in complex **1**, the monoatomic bridging mode in complexes **2** and **3**, the syn−syn bidentate bridging mode in complexes **1** and **3**, and one of the syn−syn bidentate bridging coordination modes in **2**. However, there is a significant deviation between Δ_{calcd} and Δ_{exp} values for the syn−anti bidentate bridging mode in complex **4** and one of the syn−syn bidentate bridging modes in complex **2** perhaps due to cage deformation.[30a]

Complex **1** possesses three types of acetate binding modes, whereas complexes **2**−**4** possess two. ^{1}H and ^{13}C NMR spectra of complexes **1**−**4**, however, revealed only a singlet for the acetate C*H*$_3$ protons and two singlets for O*C*(O)*C*H$_3$ carbon nuclei. The simple ^{1}H and ^{13}C NMR spectral pattern observed for complexes **1**−**4** may be ascribed to the labile nature of both Zn(II) (due to d^{10} electronic configuration)[1f,34] and acetate ligands, thus making these complexes highly fluxional in solution at ambient temperature. Lewis base coordinated Zn(II) carboxylate complexes are known for their fluxional behavior due to the "carboxylate shift" process that occurs at a rate faster than the NMR time scale. Demšar and co-workers showed that the bidentate bridging and monoatomic bridging acetates in the tetranuclear [Zn$_4$(bdmap)$_2$(μ_2-η^2:η^0-OAc)$_2$(μ_2-η^1:η^1-OAc)$_4$] (Hbdmap: 1,3-bis(dimethylamino)-2-propanol) were indistinguishable by ^{1}H NMR spectroscopy at ambient temperatures but distinguishable at 212 K.[35] Complex **1** was, therefore, subjected to a variable-temperature (VT) ^{1}H NMR spectroscopic study in THF-d_8 at 298, 278, 258, 238, and 218 K to identify three types of acetate C*H*$_3$ protons, and the resulting stack plot in the 0.0−4.0 ppm region is depicted in Figure 9. As can be seen, the ^{1}H NMR spectrum of complex **1** revealed a broad peak

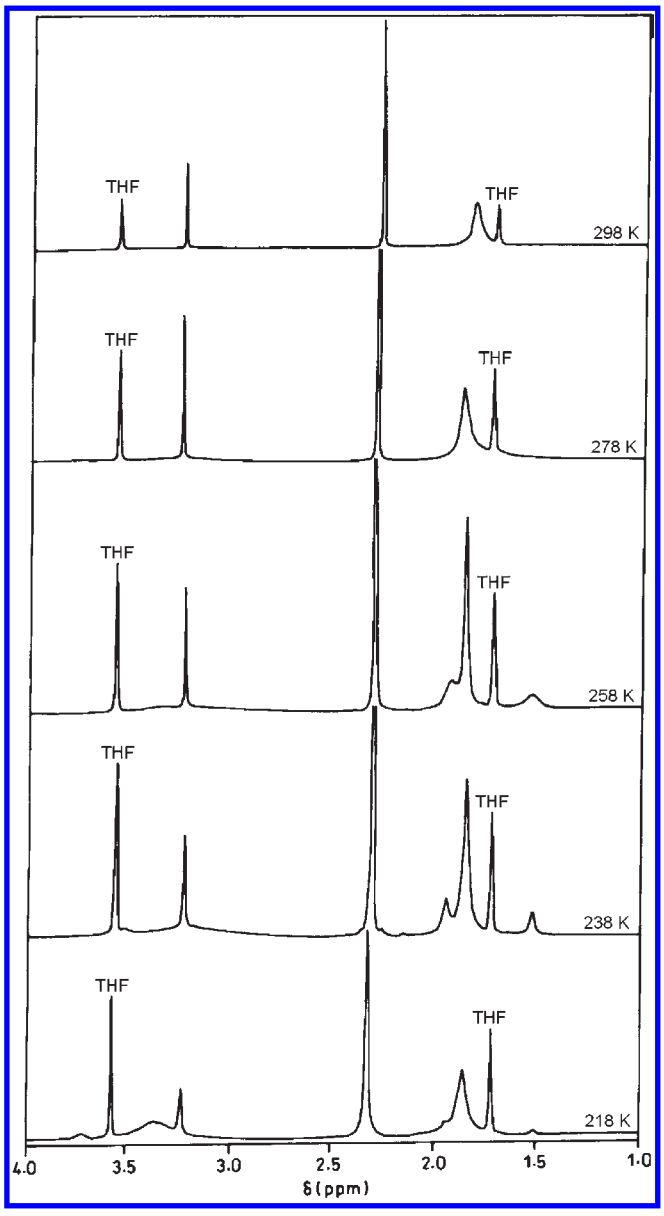

Figure 9. VT ^{1}H NMR spectrum of complex **1** in THF-d_8 at temperatures indicated suggesting partial dissociation of the sample and a rapid "carboxylate shift" process.

at δ_H = 1.83 ppm for OC(O)C*H*$_3$ protons at 298 K, but this peak decoalesces into three separate peaks at δ_H = 1.52, 1.86, and 1.96 ppm in a ∼1.00:7.45:1.70 ratio at 238 K. The THF-d_8 solution of **1** was spiked with the same solution of *N*,*N*′,*N*″-triphenylguanidinium acetate, [C(NHPh)$_3$]OAc, to better understand the observed spectral pattern. The ^{1}H NMR spectrum of the mixture after a spiking experiment revealed only one peak at δ_H = 1.86 ppm for OC(O)C*H*$_3$ protons (see the Supporting Information). Thus, complex **1** dissociates in solution to a significant extent. The signal at δ_H = 1.86 ppm for complex **1** in THF-d_8 at temperatures ≤ 258 K corresponds to the dissociated OC(O)C*H*$_3$ protons, and those signals at δ_H = 1.52 and 1.96 ppm correspond perhaps to the terminal and bridging OC(O)C*H*$_3$ protons of the undissociated complex **1**. The terminal and bridging OC(O)C*H*$_3$ protons in complex **1** are indistinguishable up to 278 K but are distinguishable below 278 K.

(33) Ishioka, T.; Shibata, Y.; Takahashi, M.; Kanesaka, I.; Kitagawa, Y.; Nakamura, K. T. *Spectrochim. Acta, Part A* **1998**, *54*, 1827.
(34) Vahrenkamp, H. *Dalton Trans.* **2007**, 4751.
(35) Demšar, A.; Košmrlj, J.; Petriček, S. *J. Am. Chem. Soc.* **2002**, *124*, 3951.

Chart 1

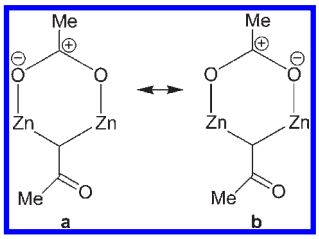

However, syn−syn bidentate bridging and the asymmetric chelating−bridging OC(O)CH_3 protons in complex **1** are indistinguishable even at 218 K, perhaps due to a rapid "carboxylate shift" process. The TOF−MS spectral data of complex **1** revealed a molecular ion peak at m/z = 801 in addition to several other species (see the Supporting Information). Thus, both VT ^{1}H NMR and mass spectral data indicated the presence of complex **1** in solution accompanied by other species resulting from a dissociative pathway.

The solution ^{13}C NMR spectra of complexes **1**−**4** revealed a single peak for the CH_3 carbon (16.0−24.0 ppm) and a single peak for the OC(O) carbon (∼180 ppm) irrespective of the types of acetate coordination modes. This artifact could be due to sample dissociation, solvent coordination, or a rapid "carboxylate shift" process. The solid-state CP-MAS ^{13}C NMR was shown to be one of the useful techniques used to distinguish various types of acetate coordination modes,[36,37] and hence we measured δ_c for complexes **1**−**4**. The solid-state CP-MAS ^{13}C NMR spectrum of complex **1** revealed four peaks at δ_c = 17.7, 19.0, 22.1, and 24.2 ppm for the CH_3 carbon as anticipated but only two peaks at δ_c = 177.2 and 180.3 ppm for OC(O) carbon instead of three. The following δ_c trend for the OC(O) carbon of the related zinc(II) acetate complexes is generally accepted in the literature: δ_C(chelating) > δ_C(bidentate bridging) > δ_C(monodentate).[36a] Further, an octahedral Zn(OAc)$_2\cdot$2H$_2$O that possess two bidentate chelating acetate and two water molecules revealed a peak at δ_c = 184.4 ppm for OC(O) carbon.[36a,38] Hence, we assign δ_c = 180.3 ppm of complex **1** for both the syn−syn bidentate bridging and the asymmetric chelating−bridging OC(O) carbon, perhaps due to the isochronous nature of OC(O) carbon nuclei or the peak may be unresolved. The relatively upfield-shifted δ_c = 177.2 ppm may be assigned for the monodentate OC(O) carbon, and this reasoning is based on the fact that two mesomeric structures **a** and **b** can be drawn for the bidentate bridging acetate, as shown in Chart 1, and hence the carbonyl carbon is more deshielded than the carbonyl carbon of the monodentate acetate. Complexes **2** and **3** revealed one signal for the monoatomic bridging [δ_c = 176.6 (**2**) and 178.6 (**3**)] and one signal for the bidentate bridging [δ_c = 178.4 (**2**) and 177.5 (**3**)] OC(O) carbon. The solid-state CP-MAS ^{13}C NMR spectrum of **4** revealed two peaks at δ_c = 177.3 and 183.0 ppm that could be assigned for the monodentate and syn−anti bidentate bridging OC(O) carbon, respectively. Further, the δ_c = 183.0 ppm assigned for the syn−anti bidentate bridging OC(O) of **4** closely matches with the δ_c values reported for anhydrous Zn(OAc)$_2$'s (δ_c = 183.2 and 184.2 ppm[37]) that possess a chemically identical but crystallographically distinct syn−anti bidentate bridging OC(O)CH$_3$ carbon, as revealed by a single-crystal X-ray diffraction study.[39] Upon comparing the δ_C values of the OC(O) carbon of complexes **1**−**4** with the related complexes in the literature,[36a] the following δ_c trend may be proposed: δ_C(chelating) > δ_C(bidentate bridging) ∼ δ_C(monoatomic bridging) > δ_C(monodentate).

Thermal Studies of Complexes 1−4. The TGA of complex **1** indicated a 4.97% weight loss (calcd weight loss: 4.50%) in the temperature range of 50−105 °C, corresponding to the loss of two coordinated water molecules. Upon further heating, CO_2 and 3,5-lutidine were lost in sequence, and at the end of a thermolysis event carried out up to 600 °C, only 6% residue was left, perhaps due to the formation of volatile species. Complexes **2**−**4** upon heating lose CO_2 and lutidine in sequence and leave no residue at the end of thermolysis, as revealed by TGA/DTA data (see the Supporting Information).

Mechanistic Aspects. The plausible mechanism for the formation of complexes **1**−**4** may be explained by invoking a point zero charge (pzc) model proposed by Ramanan and Whttingham[40] and subsequently cited by others.[41−46] According to the pzc model, as soon as a metal salt is dissolved in water or a nonaqueous solvent, a soluble metal complexes or point zero charge species is initially formed, and such soluble metal complexes undergo condensation at the isoelectric point. The manner in which condensation occurs depends upon the nature of metal salts, supporting ligands, polarity of the solvent, pH of the medium, and stoichiometry of the reagents involved. The plausible mechanism of the formation of complexes **1**−**4** based on the pzc model is illustrated in Scheme 1.

The reactions of Zn(OAc)$_2\cdot$2H$_2$O with 3,5-lutidine, 2,3-lutidine, 2,4-lutidine, or 3,4-lutidine may give rise to one or two neutral species or point zero charge species such as **X**, **Y**, or **Z**, depending upon the steric/basic properties of lutidines. The zinc in these species is likely to have an octahedral geometry.[46] Zn(OAc)$_2\cdot$2H$_2$O in the presence of 3,5-lutidine may form species **X** and **Y**, and these species could condense in an **XYX** sequence to afford complex **1**. Zn(OAc)$_2\cdot$2H$_2$O in the presence of sterically more hindered and more basic 2,3-lutidine or 2,4-lutidine may form neutral species **Y** and **Z** that could subsequently condense in a **ZYZ** sequence to afford complex **2** or **3**. However, Zn(OAc)$_2\cdot$2H$_2$O in the

(36) (a) Ye, B.-H.; Li, X.-Y.; Williams, I. D.; Chen, X.-M. *Inorg. Chem.* **2002**, *41*, 6426. (b) Ye, B.-H.; Williams, I. D.; Li, X.-Y. *J. Inorg. Biochem.* **2002**, *92*, 128.
(37) Hunt, P. A.; Straughan, B. P. *J. Chem. Soc., Dalton Trans.* **1990**, 2131.
(38) Ishioka, T.; Murata, A.; Kitagawa, Y.; Nakamura, K. T. *Acta Crystallogr.* **1997**, *C53*, 1029.
(39) (a) He, H. *Acta Crystallogr.* **2006**, *E62*, m3291. (b) Clegg, W.; Little, I. R.; Straughan, B. P. *Acta Crystallogr.* **1986**, *C42*, 1701.
(40) Ramanan, A.; Whittingham, M. S. *Cryst. Growth Des.* **2006**, *6*, 2419.
(41) Pavani, K.; Ramanan, A.; Whittingham, M. S. *J. Mol. Struct.* **2006**, *796*, 179.
(42) (a) Lan, Y.-Q.; Li, S.-L.; Wang, X.-L.; Shao, K.-Z.; Du, D.-Y.; Zang, H.-Y.; Su, Z.-M. *Inorg. Chem.* **2008**, *47*, 8179. (b) Pavani, K.; Lofland, S. E.; Ramanujachary, K. V.; Ramanan, A. *Eur. J. Inorg. Chem.* **2007**, 568.
(43) Prasad, T. K.; Rajasekharan, M. V. *Cryst. Growth Des.* **2008**, *8*, 1346.
(44) Thomas, J.; Ramanan, A. *Cryst. Growth Des.* **2008**, *8*, 3390.
(45) (a) Morris, R. E. *ChemPhysChem* **2009**, *10*, 327. (b) Shoaee, M.; Anderson, M. W.; Attfield, M. P. *Angew. Chem., Int. Ed.* **2008**, *47*, 8525.
(46) Rood, J. A.; Boggess, W. C.; Noll, B. C.; Henderson, K. W. *J. Am. Chem. Soc.* **2007**, *129*, 13675.

Scheme 1. Plausible Mechanism for the Formation of Complexes **1**−**4**

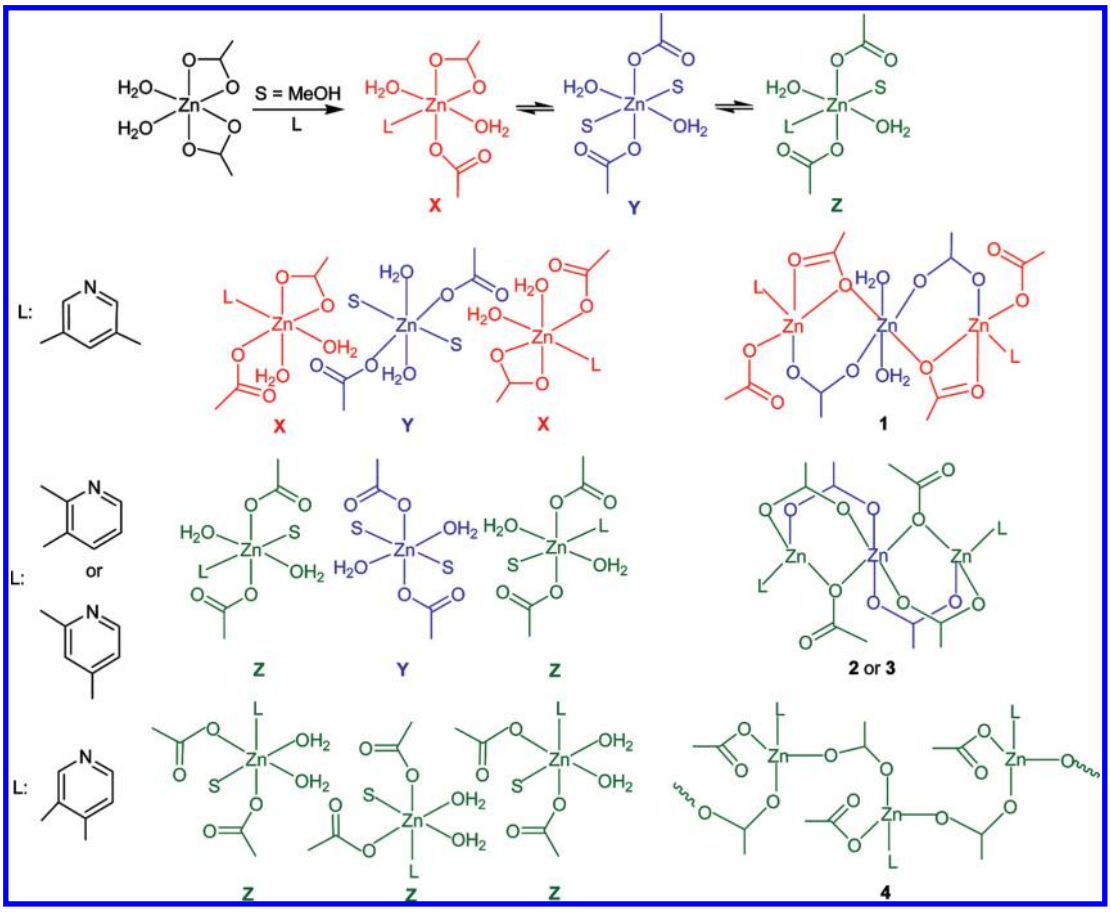

presence of more basic 3,4-lutidine may form only one species **Z**, which could subsequently condense with itself to afford a one-dimensional coordination polymer **4**. No reaction was observed between $Zn(OAc)_2 \cdot 2H_2O$ and the most sterically hindered 2,6-lutidine, indicating perhaps the absence of formation of neutral species such as **X**, **Y**, or **Z** owing to the steric bulk of the latter.

The 1:1 Zn/L ratio is maintained only in complex **4**, whereas a 3:2 ratio is maintained in complexes **1**−**3**. This observation may be related to the number and nature of the equilibrating species formed upon dissolution of the reactants in organic media, and these in turn may be influenced by basic/steric properties or both of the Lewis bases. It is difficult to delineate the individual role of steric and basic properties of Lewis bases in deciding the nuclearity/aggregation of the products, although it appears that 3,4-lutidine upon reaction with $Zn(OAc)_2 \cdot 2H_2O$ produces only **Z**, whereas sterically somewhat comparable but less basic 3,5-lutidine generates two species, namely, **X** and **Y**, from such a reaction. One of the reasons for the observed open framework in complex **1** versus the cage framework in complexes **2** and **3** underlines the significance of noncovalent interactions in the crystal lattice of the former versus increased steric and basic properties of lutidines in the latter.

Concluding Remarks

We have isolated three lutidine coordinated discrete trinuclear zinc(II) acetate complexes **1**−**3** and a one-dimensional coordination polymer **4** in good yield, and all were structurally characterized. Complex **1** represents the first structurally characterized discrete trinuclear complex that possess three distinct acetate coordination modes, namely, monodentate, bridging bidentate, and asymmetric chelating bridging, and this complex falls under class II as per the classification of Lippard and co-workers.[7] VT ^{1}H NMR data indicate that complex **1** in solution dissociates significantly, and the remaining undissociated complex **1** perhaps undergoes a "carboxylate shift" rapidly, even at 218 K. Upon comparing the structural parameters of complex **1** with those of **I**, **2**, and **3**, it can be suggested that either decreasing the basicity or increasing both the basicity and steric bulk of L shifts the acetate coordination mode from asymmetric chelating bridging to monoatomic bridging. From the present investigation, noncovalent interactions in the crystal lattice appear to play a decisive role, and subtle basic/steric properties of lutidine appear to play a supportive role in deciding the nuclearity/aggregation and acetate coordination modes, as present in complex **1**, whereas the reverse situation appears to be true in complexes **2**−**4**.

Acknowledgment. The authors acknowledge the Council of Scientific and Industrial Research, New Delhi (#01/(2076)/06 EMR-II) for financial support. Our thanks go to Prof. A. Ramanan, Indian Institute of Technology Delhi, Delhi 110 016 for useful discussions regarding the point zero charge model. NMR Research Center, Indian Institute of Science, Bangalore 560 012 is

acknowledged for variable-temperature ^{1}H NMR and solid-state CPMAS ^{13}C NMR data.

Supporting Information Available: Crystallographic data in CIF format, figures showing the solid-state CPMAS ^{13}C NMR spectra, TGA/DTA of complexes **1**−**4**, packing diagrams of complexes **2**−**4**, TOF−MS spectra of complexes **1**−**3**, and variable-temperature ^{1}H NMR spectra of complex **1** in the presence of $[C(NHPh)_3]OAc$. This material is available free of charge via the Internet at http://pubs.acs.org.